ACS OMEGA

Open Access

http://pubs.acs.org/journal/acsodf

Article

Enhancing Concrete Properties with Agave Americana Fiber Reinforcement

Houda Hachem,* Insaf Mehrez, Ramla Gheith, and Abdelmajid Jemni

Cite This: *ACS Omega* 2024, 9, 8743−8753

Read Online

ACCESS | Metrics & More | Article Recommendations

ABSTRACT: This research article explores the potential of using agave Americana fibers (AAFs) to enhance the physical and mechanical properties of concretes. The study investigates the impact of AAFs on concrete mix proportions in detail. Different concrete compositions are systematically created by integrating AAFs into them. The chemical structure, crystallinity, morphology, and tensile strength of extracted AAFs are examined, revealing a low cellulose content and a crystallinity index of around 41.34%. The microstructural analysis highlights the rough surface morphology of the extracted AAFs. The research also evaluates how AAFs affect concrete density, water uptake, and flexural and compressive strengths across various mixtures. The results show that incorporating AAFs in a horizontal position can increase the flexural resistance by up to 99% and the compressive resistance by up to 86% without chemical reactions occurring with mud−lime concrete. However, it is worth noting that using AAFs with cement can affect fiber durability due to the alkaline environment. As the alkali concentration increases, the fiber mechanical resistance decreases. Therefore, it is recommended to use AAFs with noncement concrete for improved sustainability and durability. Overall, this study advances our understanding of eco-friendly and resilient concrete materials.

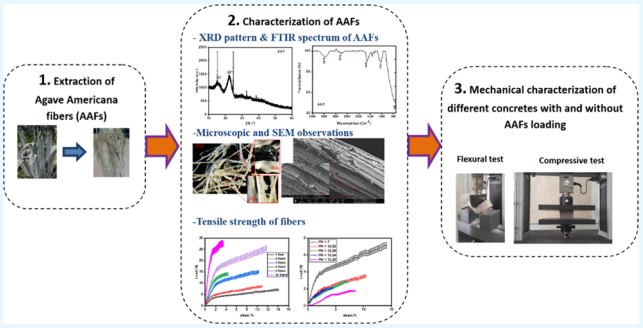

1. INTRODUCTION

In recent years, using natural fibers as reinforcements in different concretes has become increasingly popular. A more affordable, eco-friendly, and durable building material can be created by combining natural fibers with different concretes. It is important to keep in mind that the effectiveness of natural fiber depends on the volume fraction of the fiber, the strength of the bond between the fiber and matrix, fiber dispersion, and curing conditions. Studies have identified a variety of cellulosic fibers, such as jute,[1] Posidonia Oceanica,[2] sisal,[3] malva,[4] coconut,[5] palm,[6] banana,[7] bagasse,[8] and agave,[9−11] as a potential reinforcement for traditional building materials. Unlike synthetic fibers, natural fibers tend to offer superior mechanical properties while being biodegradable. These advancements have paved the way for the development of a new class of composite materials. In a study conducted by Anandh et al.,[12] sisal fibers were mixed with concrete to improve flexural and compressive strengths. However, natural fibers have been found to slow the setting time of cement composites in several experiments. Bilba et al.[8] demonstrated that natural fiber-reinforced cement composites degrade in cement concrete due to the degradation of these fibers caused by absorbed water and alkaline pore solutions, resulting from the alkaline lignin hydrolysis and partial hemicellulose solubilization in these fibers. Furthermore, the composition of the cement, including the presence of additives or chemical admixtures, can interact with natural fibers and affect the setting time. It should also be noted that adding fibers to concrete mixtures reduces their workability, which can be improved by pretreating fibers or prewetting natural fibers before adding them to mixtures.[13]

The Agave plant belongs to the Agavaceae family.[14] Two well-known types of agave fibers (AFs) are henequen, taken from Agave Forcroydes, and sisal, made from Agave Sisalana.[15] AFs are eco-friendly materials used in various industries, such as automotive and construction, due to their strong fiber-matrix adhesion, durability, and low damageability.[16] Researchers have investigated ways to improve the quality of AFs, such as chemical or mechanical treatment. For instance, Sakuri[17] found that Cantala fiber had the highest crystallinity index of 73.65% following alkali treatment with 6 h of immersion. Ali et al.[18] created new biocomposites for construction using AFs, wheat straw fibers, and cornstarch as a concrete. Their composites have thermal conductivities between 0.045 and 0.068 W/mK. Sathiamurthi et al.[19] studied the tensile and flexural character-

Received: May 25, 2023
Revised: January 21, 2024
Accepted: January 24, 2024
Published: February 13, 2024

https://doi.org/10.1021/acsomega.3c03687
ACS Omega 2024, 9, 8743−8753

istics of agave American/kenaf fiber-reinforced epoxy composites and found that the composite with 20 wt % fibers of 3 cm long had the highest tensile strength and modulus. In a study conducted by Mehrez et al.,[10] a central composite design was used to determine the ideal preparation conditions for mortar reinforced with AAFs. The best results were achieved by treating the fiber with a 4.2% concentration of NaOH and loading the composite with 17.6 wt % of AAFs. In another experiment, Deghboudj et al.[20] investigated the impact of three key parameters (fiber length, volumetric fiber percentage, and NaOH concentration) on the bending and compressive strengths of AAF-reinforced cementitious composite. According to their findings, the composite with the highest mechanical strength was made by mixing 0.5Ve% fibers, measuring 5 mm in length and treated with a 2% NaOH solution. In a study by Caballero-Caballero et al.,[21] it was discovered that increasing the presence of agave fibers led to a corresponding increase in the compressive strength of adobe-reinforced samples. Their results show an increase of 33% in compressive strength of adobe bricks that were reinforced with 1% of AFs measuring 25 mm in length.

However, it is worth noting that the durability of AFs is a significant drawback to their use. To make the fiber more durable, a protective agent is needed. Juarez et al.[9] conducted an experiment using a concentrated calcium hydroxide solution with a pH of 12.5 to create an alkaline environment and evaluate the effectiveness of protective agents in composites. Their results showed that treatment with paraffin reduced water absorption of fibers and maintained about 50% of the tensile strength and ductility even after 1 year of exposure to a humid and alkaline environment. Cisneros-Lopez et al.[22] used maleated polyethylene to treat natural fibers such as agave, coir, and pine. The findings showed that this type of surface treatment was more effective on agave and coir due to their different chemical compositions. Overall, the surface treatment improved the fiber dispersion and produced a more uniform composite morphology, allowing for greater fiber concentrations in rotational molding. Another paper[23] compared different fiber treatment modes. The findings showed that surface treatments increased the homogeneity of natural fiber composites, while maleic anhydride-grafted polyethylene produced the best mechanical gains with a 77% increase in strength and a 30% increase in stiffness.

This study aims to determine the feasibility of using natural fibers from the Agave Americana plant to create strong and environmentally friendly composites. Previous research on the use of Agave Americana Fibers (AAFs) in building composite reinforcement is limited, so further investigation is necessary to understand the effects of AAFs on different concrete compositions and properties. The introduction section discusses the challenges associated with traditional reinforcement materials and the importance of finding eco-friendly alternatives. The Materials section explains how fibers were extracted and samples were prepared, while the Methods section outlines the techniques used in this study. Results include analyses of the chemical composition, crystallinity index, microscopic observations, and tensile properties of the fibers as well as comparisons of the flexural and compressive strengths of different composites made from mud, cement, lime, and plaster with and without the addition of AAFs. The study's key findings are presented and discussed in detail.

2. MATERIALS AND METHODS

2.1. Materials. The studied composite samples were made by using cement, mud, lime, and plaster mixed with tap water. Different weight fractions of cement (C), mud (M), lime (L), and plaster (P) were mixed. Composites are prepared manually using a traditional procedure (hand mixing) and labeled based on their composition and percentage as shown in Table 1. The

Table 1. Mixture Formulations of Prepared Concrete

case	abbreviations	cement (C)	mud (M)	lime (L)	plaster (P)
1	M4L6		40%	60%	
2	C4M3L3	40%	30%	30%	
3	C4P6	40%			60%
4	C4L6	40%		60%	
5	C6P4	60%			40%
6	M3L4P3		30%	40%	30%
7	L5P5			50%	50%
8	L10			100%	
9	C4M6	40%	60%		

cement used is Portland CEM II/A-L32.5R with a bulk density of 1902 kg/m^3. The used mud has a bulk density of 1855 kg/m^3. The mud was sieved to remove large particles with very low clay content and was suitable for high-quality concrete. The grain mud used has a maximum size of 1 mm. The used lime is Portland CEM II/A-L42.5N with a bulk density of 692 kg/m^3. The plaster used is KNAUF with a bulk density of 1104 kg/m^3.

There are several methods to process agave fibers, including retting, scraping, and mechanical extraction. These techniques are used to get rid of the waxes, oils, and other impurities from the fibers' surface, creating a more uniform and cleaner material. In this study, Agave Americana leaves are gathered from a Tunisian forest. The thorns on the end and lateral sides were removed by using a sharp knife. The leaves were divided horizontally into pieces and submerged in water for 15−20 days in a container to remove fibers. The same extraction method was explained in ref 24. This method consists of the submersion of the agave leaves in a tank with 37 °C water for many days until fibers are dignified and nonadherent. Then, AAFs are taken from the water and carefully rinsed with tap water to eliminate the odor and froth. Then, they were dried in the sun for 5 days (see Figure 1). The composite processing involved removing damaged and unwanted fibers and slicing Agave Americana fiber before use. For this study, AAFs were utilized as reinforcements for nine different matrices, as described in Table 1, with each composite containing a 20% volume ratio of fibers. To prepare the samples, a homogenized mixture was manually poured into a parallelepiped mold of 16 × 16 × 4 cm^3 according to ASTM D790-10.[25] The AAFs were then installed horizontally within the composite samples and were used in a wet state to make them more flexible. Once unloaded, the fibers could deform and then return to their original state. After 24 h, all samples were carefully removed from the mold and conserved for 28 days in laboratory conditions. The water and concrete ratio by weight, W/C, is fixed to 0.8 for all composites (with and without fiber). Three samples for each mechanical test are prepared.

2.2. Methods. *2.2.1. Fourier Transform Infrared Spectrometry Analysis.* Fourier transform infrared spectrometry (FTIR) is a technique used to investigate the chemical composition and molecular structure of materials. It relies on the interaction of infrared radiation with a sample. When

https://doi.org/10.1021/acsomega.3c03687
ACS Omega 2024, 9, 8743−8753

Figure 1. Agave Americana (a) and plant (b) extracted fibers.

infrared light passes through a sample, certain chemical bonds within the sample absorb specific frequencies of light. The resulting absorption spectrum provides information about the functional groups and chemical bonds present in the material. FTIR spectroscopy was conducted to assess the chemical structure of used materials (cement, mud, lime, plaster, and AAFs). A PerkinElmer Spectrum BX Model spectrophotometer is the apparatus in use. There are 15 scans in the accumulation count, and the spectral range encompasses the 400−4000 cm^{-1} gap. Chemicals were identified based on previously published information in the literature.

2.2.2. X-ray Diffraction Analysis. X-ray diffraction (XRD) is a technique used to analyze the crystallographic structure of materials. It involves directing a beam of X-rays at a crystalline sample, and the X-rays interact with the crystal lattice, causing them to disperse. By measuring the angles and intensities of the distributed X-rays, XRD provides information about the spacing of the lattice planes within the crystal structure. This information allows researchers to determine the crystal structure, unit cell dimensions, and orientation of crystal grains in a material. XRD is utilized to analyze AAFs' atomic structure and phase compositions using a Bruker D8 advanced diffractometer. Cu−K radiation was used to scan the fiber from 10 to 50 °C with steps of 0.020 °C at an ambient temperature, using 40 kV and 40 mA. To calculate the crystallinity index (CI) of AAFs, the procedure outlined by Wang et al.[26] was adopted

$$\mathrm{CI}\ (\%) = \frac{\sum A_{\mathrm{cryst}}}{A_{\mathrm{tot}}} \times 100 \tag{1}$$

2.2.3. Microscopic Observation. Microscopic observation is a crucial technique used to examine the contents of extracted

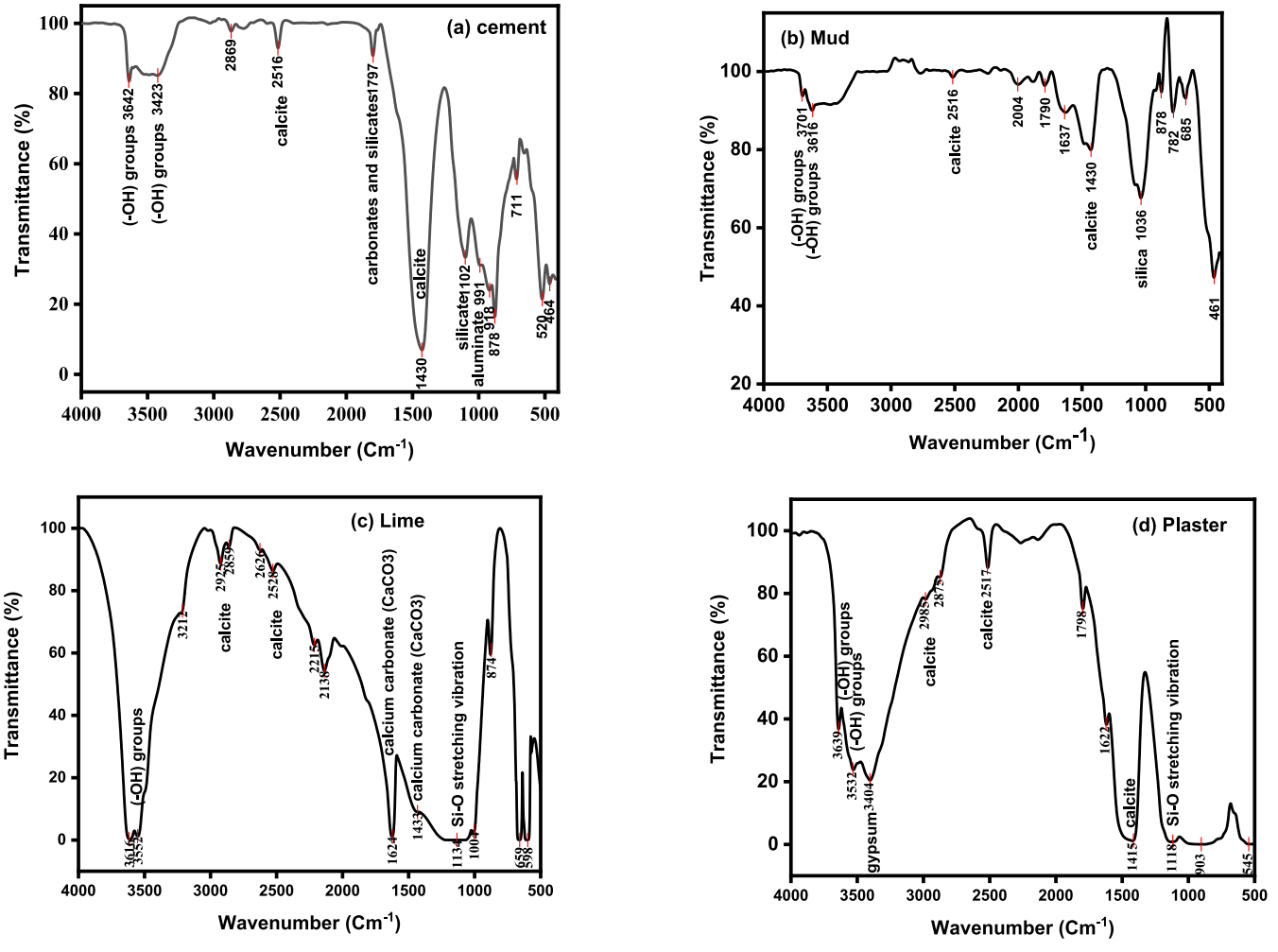

Figure 2. FTIR spectrum of used (a) cement, (b) mud, (c) lime, and (d) plaster.

https://doi.org/10.1021/acsomega.3c03687
ACS Omega 2024, 9, 8743−8753

agave fibers for a comprehensive analysis. The examination process utilizes a Zeiss Stemi 2000-C Stereo binocular magnifier with a zoom range of 6.5−50. To prepare the specimens for observation, the AAFs are evenly dispersed on a microscope slide, ensuring that they are well-distributed and not clumped together. This step is essential for an accurate and representative analysis. Once the specimens are ready, microscopic observation is carried out using a Zeiss magnifier. This involves setting up the microscope, placing the slide on the stage, adjusting the magnification level within the zoom range, focusing to bring the fibers into clear view, and capturing images. During the examination, various characteristics of the AAFs, such as fiber type, size, and morphology, are meticulously examined and recorded. The data collected during this process are crucial for characterizing and identifying AAFs used to prepare building composite samples.

2.2.4. Scanning Electron Microscope (SEM). The morphology of the AAFs and the concrete surfaces is examined using the scanning electron microscope (SEM) and SEM ZEIXX field emission. Silver plates were used to fix the composite samples. In a vacuum chamber, they were then covered with a small layer of gold to make them conductive and ensure proper analysis.

2.2.5. Water Uptake Testing of Composites. Tests for water uptake followed the ASTM D570. The sample was weighed dry (w_0), then immersed in water, and weighed wet (w_t) after removing trapped water on a filter paper. Water uptake (H) was calculated using these measurements as follows[27]

$$H\ (\%) = \frac{w_t - w_0}{w_0} \times 100 \tag{2}$$

2.2.6. Density Determination of Composite. The apparent density is defined as the ratio of the weight by volume. The composite samples were dried in a controlled oven at 70 °C until they were of constant weight. After that, the samples were weighed using an electronic balance with a precision of roughly 10^{-4} g. A caliper with a precision of roughly 0.02 mm was used to measure the dimensions of the samples.

2.2.7. Mechanical Behavior of Composites. The EZ 50 kN machine was used to test the flexural and compressive strengths at a speed loading of 5 mm/min. During the flexural test, a load is applied to the transversal segment of the sample. The flexural (R_f) and compressive (R_c) strengths are calculated as follows

$$R_f = \frac{3Fl}{2bh^2} \tag{3}$$

$$R_c = \frac{F}{A} \tag{4}$$

Three measurements are conducted to obtain the average of three data of measurement.

3.5.3. Tensile Strength of AAFs. The tensile tests were conducted according to the ASTM standard D3217-79[28] using a Lloyd LRX Plus universal tension/compression machine with capacities up to 2.5 kN. The latter was adjusted to a speed of 10 mm/min for a 50 mm specimen length to respect the test duration of 20 ± 3s specified in the NFG 07002 French Standard. The tensile strength (T_S) of the used AAFs was calculated as follows

$$T_S = \frac{P}{bh} \tag{5}$$

where P is the load (kN), b is the width of a sample (mm), and h is the height of the sample (mm).

3. RESULTS AND DISCUSSION

3.1. FTIR Spectra of the Used Concretes. Figure 2 presents the results of FTIR spectroscopy used to analyze the bonding and functional groups present in cement (2.a), plaster (2.d), lime (2.c), and mud (2.b) used in construction. Various spectra have been included to enable a more comprehensive analysis of the fundamental differences among the various types of concrete studied. These spectra serve as a tool for identification and qualitative quantification, taking into account the nonlinear relationship between intensities and fractional content. By comparison of the FTIR spectra of various concretes, a deeper understanding of the chemical composition, functional groups, and bonding patterns in these construction materials can be gained. Upon comparing the data, it is evident that the intensity of peaks for the stretching vibration of the O−H and HOH groups is higher in plaster and lime compared to cement and mud. This heightened intensity suggests that lime and plaster exhibit a high hydrophilic character. In lime production, limestone or calcium carbonate undergoes calcination, forming calcium oxide (CaO). When water is added to lime, a chemical reaction called slaking occurs, creating calcium hydroxide ($Ca(OH)_2$). This compound is rich in the HOH and O−H groups, contributing to its alkalinity and hydration characteristics. Plaster, typically made from gypsum (calcium sulfate dihydrate), also contains a significant amount of HOH groups due to the presence of water molecules in its crystal structure. The abundance of these groups signifies the hydrophilic nature of the plaster, indicating its capacity to readily interact with water during various construction processes.

3.2. FTIR Spectrum of AAFs. Figure 3 displays the extracted AAFs' FTIR spectrum, revealing their molecular composition by

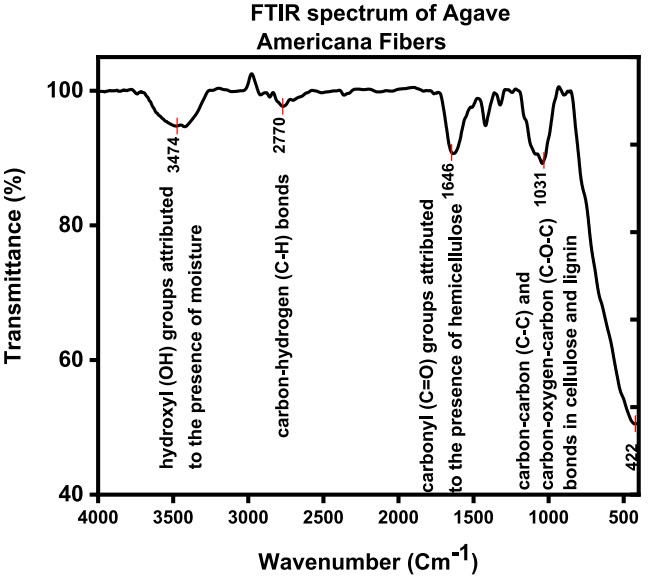

Figure 3. FTIR spectrum of AAFs.

identifying specific chemical bonds and molecular vibrations. The peaks observed at 3425 and 1043 cm^{-1} correspond to notable stretching vibrations associated with the O−H and C−O, respectively. These peaks signify the presence of hydroxyl (O−H) groups and carbonyl (C−O) groups within the fiber structure. Furthermore, the absorptions observed at 1423 and 1320 cm^{-1} are attributed to the stretching vibrations of the C−

https://doi.org/10.1021/acsomega.3c03687
ACS Omega 2024, 9, 8743−8753

H, O−H, and CH_2 groups, elucidating the composition of the fiber constituents. These groups are integral to the fiber's molecular structure and contribute to its chemical properties. The peak observed at 1632 cm^{-1} indicates the presence of water absorption in cellulose-based materials. It is important to note that the intensity of the signal for AAFs in this spectrum is notably lower than those of other fiber types that have been documented in the literature. This validates the low cellulose content in AAFs. It highlights their unique composition compared to other fibers.[29]

3.3. X-ray Diffraction (XRD) Patterns of AAFs. Figure 4 displays the XRD patterns of AAFs, which demonstrate unique

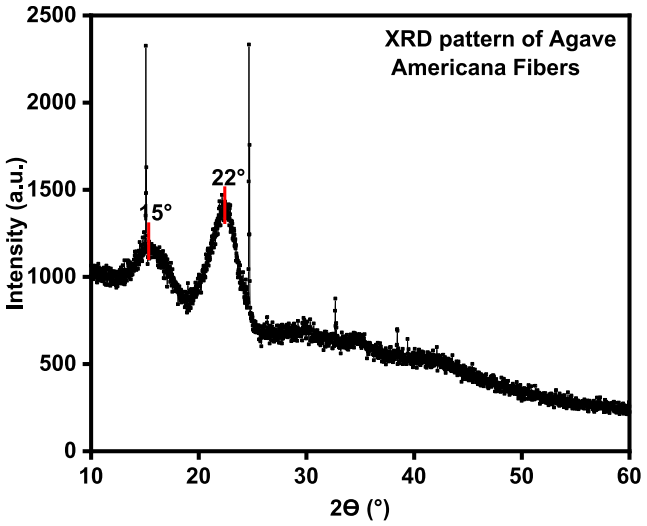

Figure 4. XRD patterns of AAFs.

crystal structures within the fibers. These patterns offer significant information about the fiber's composition, polymorphic forms, or specific mineral phases. Consequently, they can aid in the characterization of the fibers and assist in comprehending their physical properties, mechanical strength, and potential applications. In the XRD patterns, two prominent peaks were observed at θ = 15 and 22°, corresponding to the (101) and (002) crystalline planes, respectively.[10] These peaks signify a well-defined crystallographic orientation within the fibers. To quantify the crystallinity of AAFs, eq 1 was utilized, resulting in a calculated crystallinity index of approximately 41.34%. Comparing this index with other fibers documented in the literature, the crystallinity index of AAFs was found to be similar to that of Posidonia leaves[2] and higher than that of wood.[27] This comparison underlines the distinct crystalline nature of AAFs in comparison to those of other natural fibers. It is crucial to understand that the physical, mechanical, and chemical properties of materials that use AAFs as reinforcement are highly dependent on the crystallinity of the fibers. Fibers with higher crystallinity tend to result in harder materials due to the more organized arrangement of atoms. Therefore, the higher crystallinity of AAFs may offer potential benefits in improving the hardness of materials when used as a reinforcing agent.[30]

3.4. Microscopic and SEM Observations of AAFs. Figure 5 shows the microscopic observation of AAFs that were viewed using a binocular magnifier at two different magnifications. By making this observation, the microstructural characteristics of the fibers can be analyzed. Upon examination using a 20× magnification, it was discovered that the particle size distribution of the AAFs used was not uniform. When viewed under a 50× magnification, microfibrils can be seen in agave fibers. The diameter of these fibers varies greatly, ranging from thin filaments measuring around 5−10 μm to thicker strands with diameters of 100 μm or more. The AAF fibers' surface has a structure similar to other natural fibers, consisting of multiple elementary fibers connected by pectin and other noncellulosic materials.[31] Additionally, there may be visible contaminants on the fibers' surface. To improve interfacial adhesion with cement matrix and remove contaminants, natural fibers often undergo chemical treatments.[32]

In order to gain a better understanding of the structure and surface properties of agave fibers, SEM observation was conducted to gather more information about the AAFs. This in-depth analysis is crucial for advancing research on agave fibers and exploring their potential applications in sustainable materials and composites. Figure 6 displays the SEM observation results of AAFs. The shape of AAFs is cylindrical, and they consist of microfibrils arranged in a line-like pattern. The fiber's surface also contains significant amounts of waxes, oils, and other impurities. Due to its rough surface structure, AAFs are a promising material for creating biomaterials that are efficient and have low density. In summary, AAFs are considered hard fibers that have unique morphological, physical, mechanical, and chemical properties when compared to other fibers.

4.5. Tensile Resistance of AAFs. Agave Americana fibers' tensile properties were evaluated by testing 1−10 fibers in Figure 7. The overall tensile strength of multiple fibers is higher than that of individual fibers because they distribute force more efficiently. The tensile strength of a single agave fiber is 7.12 N; when 10 fibers are bundled, the strength increases to about 24 N. Each curve has three zones: a linear zone with immediate elastic mechanical relaxation, a viscoelastic deformation zone with a small increase of stress, and a plastic deformation zone that causes fiber rupture. The stress−strain curves of fibers 1, 2, 3, 4, and 5 are similar in form to the curve obtained by Msahli et al.[33] The tests for these fibers were stopped at their maximum values of strain, and no drop in load was observed after the end point. However, the stress−strain curve of 10 fibers underwent alteration due to sliding as they were pulled from both ends, which were strongly affixed to the grips of the tensile testing machine. The tensile strength of a material refers to the maximum amount of tensile stress that can take before failure. The decision to terminate the tests at these specific end points was made purposely to explore the upper limits of strain tolerance for individual and multiple agave fibers. Table 2 shows further experimental results. In summary, agave fibers have a relatively low tensile strength when taken individually, but when several fibers are combined into a bundle, their overall strength increases significantly. This characteristic makes agave fibers useful for various applications.

4.6. Density and Water Uptake of Building Composites with and without AAF Loading. It appears that the decrease in density in all concretes after introducing AAFs is due to the lower density of the fibers in comparison to the concretes (as shown in Figure 8). Agave Americana fibers reduce the density of the composite by displacing concretes and creating voids within the structure. This results in a lower overall density and mass.

AAFs increase water uptake in concrete because of their hydrophilic nature (Figure 9). These fibers create pathways for water to penetrate the composite, acting as channels that draw

https://doi.org/10.1021/acsomega.3c03687
ACS Omega 2024, 9, 8743−8753

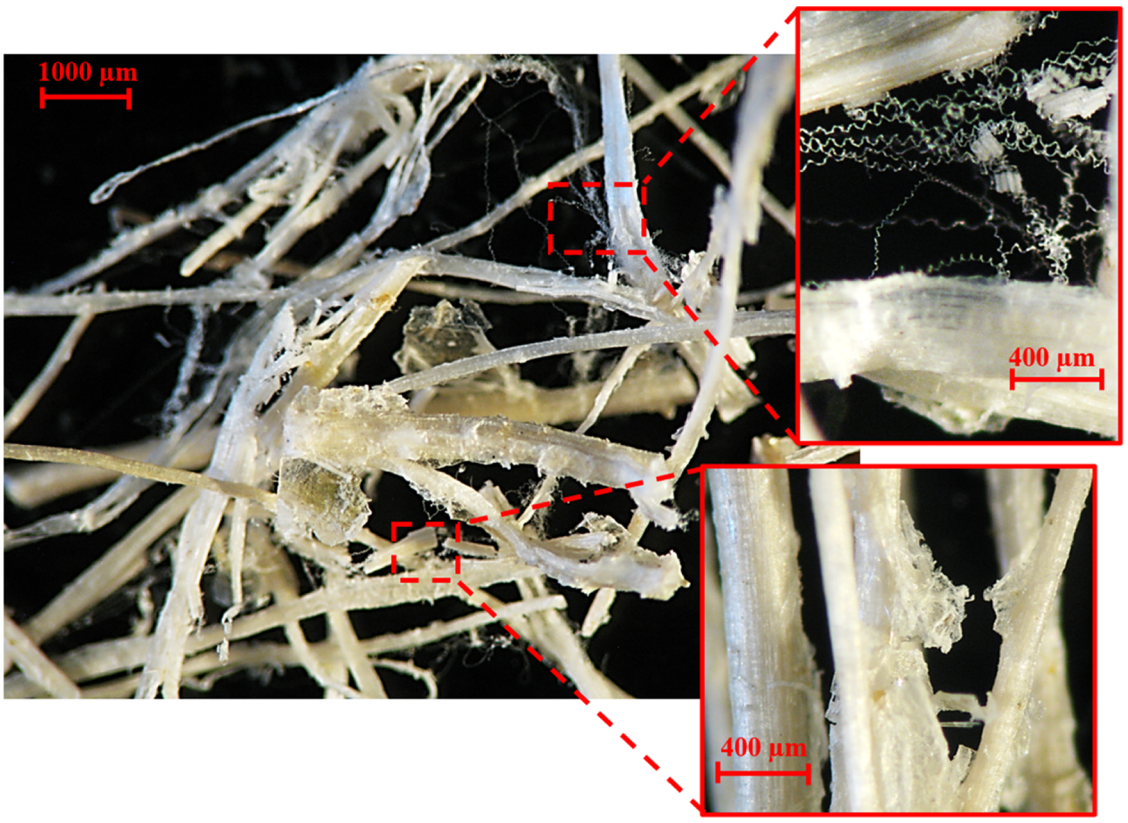

Figure 5. Binocular magnifier observation of extracted Agave Americana fibers.

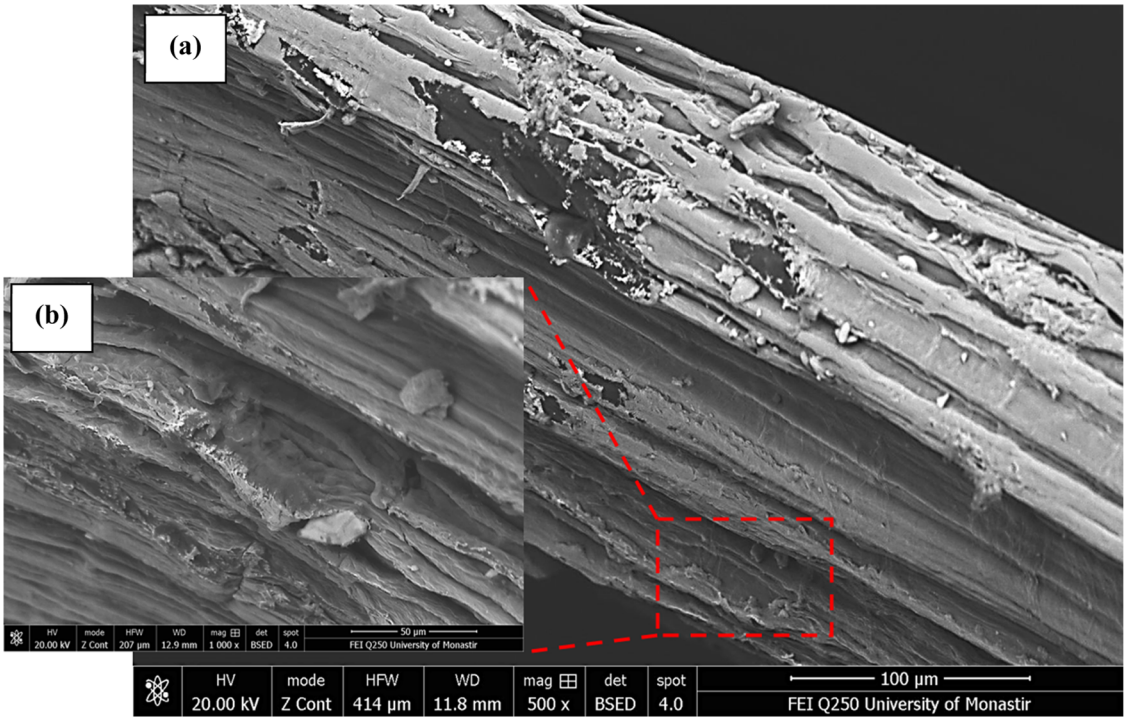

Figure 6. SEM visualization of Agave Americana fibers (a) 100 μm and (b) 50 μm.

water into the concrete−fiber mixture. This leads to a higher overall water uptake than using just the concrete material alone.

The error bars for both density and water absorption uptake were generated by using the same data replication process. Three independent measurements were taken for each case, and the results were used to calculate the error bars. These error bars show the variability in both the density and the water absorption data. To better visualize the level of uncertainty associated with these measurements, the error bars were integrated into the figures.

https://doi.org/10.1021/acsomega.3c03687
ACS Omega 2024, 9, 8743−8753

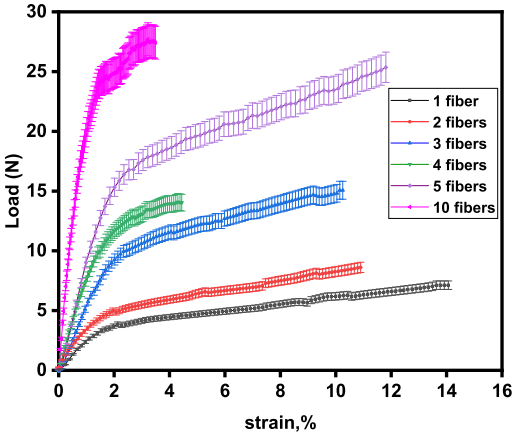

Figure 7. Stress−strain curves of 1−10 fibers.

Table 2. Experimental Results of Tensile Tests from 1 to 10 Fibers

number of agave fibers	load at break (N)	percentage of strain at break (%)	load at maximum load (N)	extension at maximum load (mm)	stiffness (N/m)
1	7.12	14.178	7.1	7.3725	5982.6
2	5.28	10.89	8.6	5.7578	10019.0
3	11.52	10.14	15	5.3726	11973.0
4	17.88	4.44	26.6	8.7151	20717.0
5	21.65	11.8	27.7	1.6763	63251.0
10	24.09	3.49	32.9	1.4320	54101.0

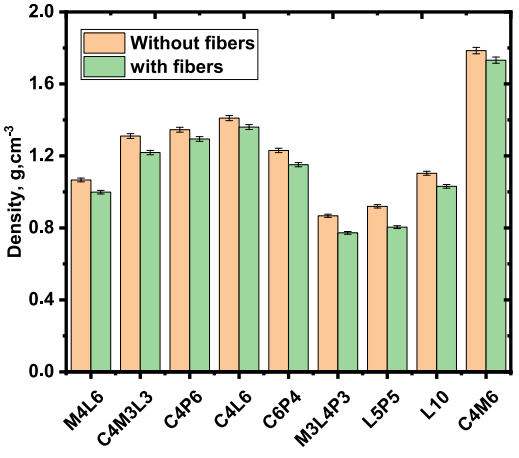

Figure 8. Density of different concrete mixtures before and after AAF loading.

4.7. Flexural and Compressive Resistance of Samples with and without AAF Loading. Testing different concretes provides a baseline for comparison and helps identify the most appropriate matrix to enhance with agave fibers. This ensured optimal performance and mechanical properties for the composite material. The flexural and compressive strengths of the tested concretes before and after AAF loading are displayed in Figures 10 and 11, respectively. Samples with lime or plaster have lower mechanical strength compared with cement and mud. This is due to differences in their compositions, densities, and intended applications. Before AAF loading, all samples except (C4M6) had very low flexural and compressive strengths. Each material has its own set of advantages and is suitable for specific construction purposes.

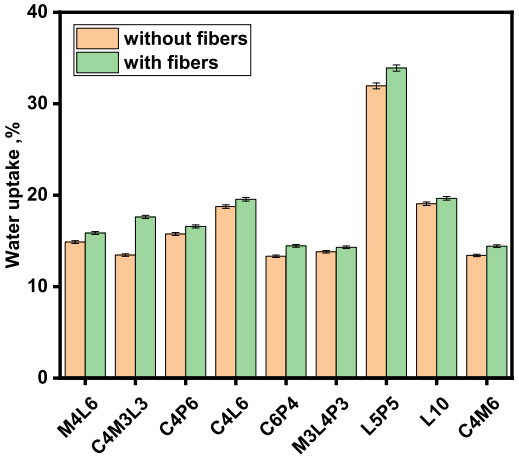

Figure 9. Water uptake of different concrete mixtures before and after AAF loading.

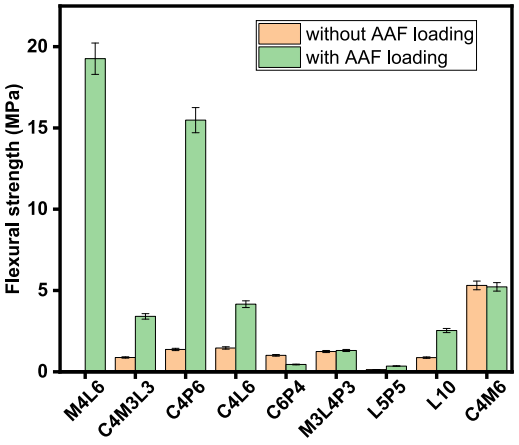

Figure 10. Flexural strength of different concretes before and after AAF loading.

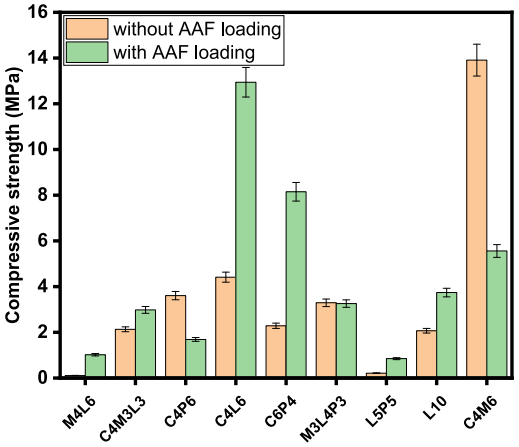

Figure 11. Compressive strength of different concretes before and after AAF loading.

Samples reinforced with AAFs showed higher flexural strengths compared to nonfibrous matrix, except for (C4M6) and (C6P4) samples. The samples' lower mechanical qualities may be due to their increased hydrophilic character, as water affects their strength, stability, bonding, and resistance to degradation.

https://doi.org/10.1021/acsomega.3c03687
ACS Omega 2024, 9, 8743−8753

The (M4L6) sample showed the highest increase in flexural strength, from 0.02 MPa (without AAFs) to 19.2 MPa (with AAFs). In Figure 12, during the flexural test of (M4L6), there is a

Figure 12. Flexural strength test of (M4L6) concrete reinforced with horizontal AAF fibers.

clear mechanical resistance of the sample loaded with AAFs. In fact, fibers in a horizontal position increased the flexural resistance (until 99%) and the compressive resistance (until 86%) without undergoing chemical reactions with the (M4L6) concrete. Agave fibers have a strong bond with the mud−lime matrix, which enormously increases its resistance to compression and flexion. Proper alignment of the fibers can prevent crack propagation and improve the overall performance of the (M4L6) concrete.

When added to the (C4M3L3) sample, agave fibers can increase compression strength by 28.4% and flexural strength by 74.14%. The addition of cement to the matrix composition without fibers can further enhance strength. The presence of 40% cement inside the (C4M3L3) concrete limits the increase of mechanical properties compared to those inside the (M4L6) concrete. It is important to have a strong interaction between the fibers and the matrix to achieve maximum strength enhancement. However, it is also important to undergo no chemical reactions between the fiber and the concrete.

Adding AAFs to cement reduces the compressive strength in (C4P6) and (C4M6) concretes but increases it for all other concretes. The (C4L6) concrete shows the highest increase in compressive strength, while (C4M6) shows the highest decrease. Flexural strength improvement is more significant for (M4L6) and (C4P6), while (C4L6), (M3L4P3), (L5P5), and (L10) show relatively similar results for both compressive and flexural strength improvement. The use of AAFs with noncement matrix is desirable as natural fibers and synthetic polymers degrade in the alkaline environment of the cement matrix.

The concrete (C4M6) has the highest flexural and compressive strengths compared with other samples before AAF loading. It contains 40% cement and 60% mud, making it stronger than mud-based materials such as adobe or cob. Figure 13 shows the compressive and flexural strengths of the concrete (C4M6) after 7, 14, and 28 days. As expected, the strength of the composite improves with age. The compressive strength of a concrete mixture that reaches around 12 MPa after 28 days is

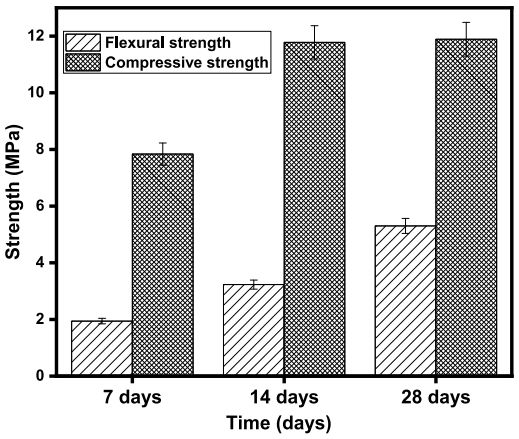

Figure 13. Flexural and compressive strengths of (C4M6) without fiber loading.

significantly low compared to that of 42.5-grade cements and even lower than 32.5-grade cement, which is nearly three times higher. This indicates a significant underperformance relative to international standards, particularly ISO-1920-4. Three factors can account for this low compressive strength. First, the use of lower-grade cement. Second, the water−cement ratio used in this experimental work is about 0.8. The excess of water dilutes the cement paste, which leads to a weakening of the strength. Third, the proportions of cement in the mixture are very poor, only 40% compared to the mud component of about 60%. Thus, improper ratios of these components can lead to low strength.

Figure 14 displays SEM images of the fractured surface of the (C4M6) sample before and after reinforcement with AAFs. The images were taken to examine the porosity and bonding of AAFs to the concrete after a flexural mechanical test. Based on Figure 14a, it is evident that the composite is nonuniform due to the presence of mud. The nonfibrous matrix displays a solid structure, indicating a good interaction between cement and mud. In Figure 14b, the samples show a nonuniform fiber distribution. The morphology of AAF surfaces appears changed with weakened and easily broken fibers. A chemical reaction between cement and AAFs results in the formation of pores on the AAF surfaces, leading to rapid degradation. Large pores resulting from the pull-off of AAFs were observed, contributing to the sample's lack of strength. This weakness is attributed to the fibrous matrix structure, which exhibits increased debonding between the matrix−fiber surface, fiber pullouts, fiber fracture, matrix fissures, and cracks in the case of concrete reinforced with AAFs.

The use of agave fibers in a mortar based on Portland cement can pose challenges regarding the chemical and physical degradation of the fiber. Portland cement is a commonly used construction material known for its high PH in the range of 12−13. The PH of cement-based materials can vary depending on several factors, including the specific composition of the cement and any additives present. This high pH is due to the presence of calcium hydroxide in the interstitial solution of the cement. When agave fibers are exposed to a high pH interstitial solution, several degradation processes can occur. The high pH can also affect the physical properties of the agave fiber. It can cause softening, loss of strength, and deterioration of the fibrous structure, reducing its ability to reinforce the mortar.

4.8. Durability of Fibers in an Alkaline Environment. In cement-based mixtures, vegetable fibers have limitations,

https://doi.org/10.1021/acsomega.3c03687
ACS Omega 2024, 9, 8743−8753

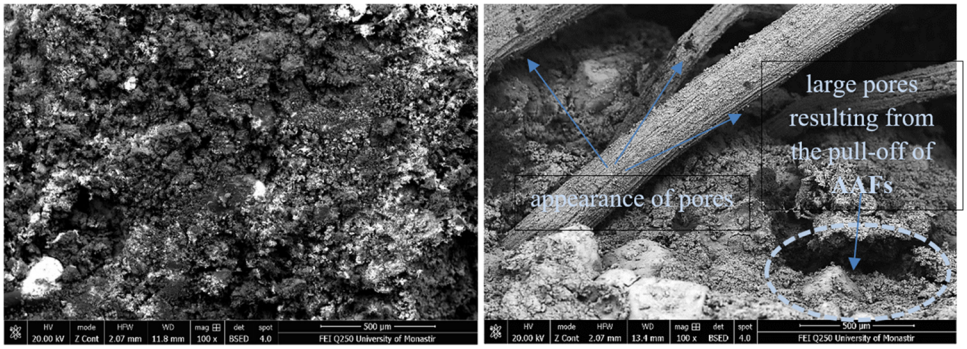

Figure 14. SEM visualization of the (C4M6) sample (a) before and (b) after AAF loading.

especially when it comes to their durability and compatibility with concretes. Most natural fibers, especially those of vegetable origin, tend to weaken in alkaline environments. They can easily deteriorate in the alkaline environments found in cement compounds due to their individual filaments that can separate.[34] Over time, a mineralization process may also occur, which can reduce the composite's strength and durability.[35] Moreover, the volume changes of porous vegetable fibers surrounded by the cement matrix can cause significant degradation at the interface of the exposed composites. Stapper et al.[36] discovered that the performance of the fibers was not correlated with the alkalinity of the surrounding environment. Instead, they observed that only hemicellulose was susceptible to rapid degradation under highly alkaline conditions. As a result, the researchers concluded that alkaline hydrolysis is not the primary factor contributing to the degradation of natural fibers in this context. According to Faruk et al.,[37] the moisture level in plant-based fibers has a significant impact on their mechanical properties and performance within composites. Li et al.[38] also stated that the strength and rigidity of natural fibers depend on the amount of cellulose present and the arrangement of microfibrils within the cell wall. In addition, the mechanical properties of natural fibers are affected by the method used for fiber extraction.[39]

This section aims to investigate the impact of an alkali environment on the mechanical performance of Agave Americana fibers. To test the durability of these fibers in concrete's alkaline environment, five sodium hydroxide (NaOH) solutions with different concentrations (0%, 4%, 7%, 9%, 10%) were prepared by dissolving the appropriate amount of NaOH in distilled water at room temperature. Agave fibers were soaked in these solutions for 24 h before being rinsed with clean water to remove any trace of NaOH. The fibers were then dried in the sun before being subjected to a single-fiber tensile test to determine their mechanical strength.

Figure 15 illustrates the relationship between the applied load and strain of soaked fibers at various pH levels. The pH values were measured using a pH meter and were found to be 7, 12.52, 12.99, 13.04, and 13.25 for NaOH solutions of 0, 4, 7, 9, and 10% by weight, respectively. The results showed that fibers exposed to high pH levels (pH > 12) support a lower load compared to those exposed to lower pH levels (pH = 7). As alkali concentration increased, fiber mechanical resistance decreased. This experiment provides insights into the resistance of vegetable fibers in an alkaline environment and important information for their use in various industrial applications, especially when incorporated with concrete. This can explain the significant degradation in mechanical strength observed in

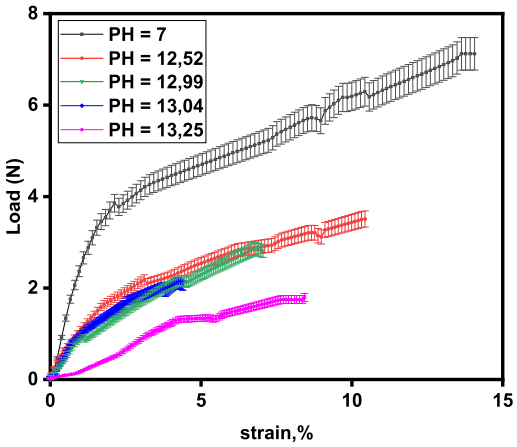

Figure 15. Stress−strain curves of one fiber under alkali solutions.

cement-based composites reinforced with AAFs, as shown in the previous section. This degradation can be attributed to the damage at the matrix−fiber interface caused by the volume change of the porous vegetable fibers within the concrete.

5. CONCLUSIONS

The use of Agave Americana fibers (AAFs) has shown promising results in enhancing the performance of building composites. These materials are stronger and lighter than the traditional ones. In particular, noncement concretes have demonstrated significant improvement in compressive and flexural strengths due to the incorporation of AAFs. The experiments conducted revealed the underlying mechanisms of this improvement. FTIR analysis of AAFs showed crucial molecular characteristics, with discernible peaks indicating the presence of O−H, C−O, and relevant functional groups. AAFs have less cellulose content compared with other natural fibers, which contributes to their effectiveness in reinforcing building materials. XRD patterns revealed distinctive crystal structures in AAFs, promising heightened material hardness. It is important to note that the effectiveness of AAFs in reinforcing is influenced by the properties of the concrete matrix, particularly its alkalinity, and the chemical compatibility between the fiber surface and concrete components. The combination of noncement matrices with AAFs yielded remarkable improvements in the strength properties of samples. Adding AAFs to lime and plaster increases their strength. However, AAF reinforcement weakens cement concrete. Agave Americana plants are valuable resources in construction. They offer many possibilities for the optimization

https://doi.org/10.1021/acsomega.3c03687
ACS Omega 2024, 9, 8743−8753

of building materials. More research is needed to minimize natural fiber degradation. Treating agave fibers can enhance their resistance to chemical degradation. Future studies will focus on impregnation with hydrophobic or chemical strengthening agents to reduce the sensitivity to alkaline environments. Using cements with a reduced alkali content can also help. However, it is important to note that the pH can change over time, so future research will focus on protection agents or inhibitors to prevent agave fiber degradation in alkaline environments.

AUTHOR INFORMATION

Corresponding Author

Houda Hachem − *Energy Research and Technology Center (CRTEn), Hammam-Lif 2050, Tunisia;* orcid.org/0000-0003-2534-0629; Email: Houda.Hachem@crten.mesrs.tn

Authors

Insaf Mehrez − *National Engineering School of Monastir (ENIM), LESTE Laboratory, University of Monastir, 5019 Monastir, Tunisia*

Ramla Gheith − *National Engineering School of Monastir (ENIM), LESTE Laboratory, University of Monastir, 5019 Monastir, Tunisia*

Abdelmajid Jemni − *National Engineering School of Monastir (ENIM), LESTE Laboratory, University of Monastir, 5019 Monastir, Tunisia*

Complete contact information is available at: https://pubs.acs.org/10.1021/acsomega.3c03687

Notes

The authors declare no competing financial interest.

ACKNOWLEDGMENTS

The authors thank Professor Hassen Abdallah from the Energy Research and Technology Center (CRTEn, Hammam-Lif, Tunisia) for providing the binocular magnifier used during the observation.

NOMENCLATURE

A	across section (mm^2)
A_{tot}	the sum of the areas under all of the diffraction peaks
$\sum A_{cryst}$	the sum of the areas corresponding to the major important crystalline peaks from cellulose I
b	the width of the test sample (m)
CI	the crystallinity index (%)
F	the average applied force (N)
h	the thickness of the test sample in the direction of bending (m)
l	support span (l = 0,1m)
R_c	compressive strength (MPa)
R_f	the flexural strength (MPa)

ABBREVIATIONS

AAFs	Agave Americana fibers
AFs	agave fibers
FTIR	Fourier transform infrared spectrometry
XRD	X-ray diffraction

REFERENCES

(1) Ahmad, J.; Arbili, M. M.; Majdi, A.; Althoey, F.; Farouk Deifalla, A.; Rahmawati, C. Performance of concrete reinforced with jute fibers (natural fibers): A review. *J. Eng. Fibers Fabr.* **2022**, *17*, No. 15589250221121871.

(2) Mehrez, I.; Hachem, H.; Gheith, R.; Jemni, A. Valorization of Posidonia-Oceanica leaves for the building insulation sector. *J. Compos. Mater.* **2022**, *56*, 1973−1985.

(3) Ouakarrouch, M.; El Azhary, K.; Mansour, M.; Laaroussi, N.; Garoum, M. Thermal study of clay bricks reinforced by sisal-fibers used in construction in South of Morocco. *Energy Rep.* **2020**, *6*, 81−88.

(4) Lima, T. E. S.; Júnior, L. T.; Nascimento, L. F. C.; Demosthenes, L. C. C.; Monteiro, S. N.; Azevedo, A. R. G. Evaluation of the feasibility application of Malva fibers in cement-based composites. *J. Mater. Res. Technol.* **2023**, *23*, 6274−6286.

(5) Tolêdo Filho, R. D.; Scrivener, K.; England, G. L.; Ghavami, K. Durabilityof alkali-sensitive sisal and coconut fibres in cement mortar composites. *Cem. Concr. Compos.* **2000**, *22* (2), 127−143.

(6) Boumhaout, M.; Boukhattem, L.; Hamdi, H.; Benhamou, B.; Nouh, F. A. Thermomechanical characterization of a bio-composite building material: Mortar reinforced with date palm fibers mesh. *Constr. Build. Mater.* **2017**, *135*, 241−250.

(7) Mostafa, M.; Uddin, N. Effect of banana fibers on the compressive and flexural strength of compressed earth blocks. *Buildings* **2015**, *5* (1), 282−296.

(8) Bilba, K.; Arsene, M. A.; Quensanga, A. Sugar cane bagasse fibre reinforcedcement composites. Part I. Influence of the botanical components of bagasse on the setting of bagasse/cement composite. *Cem. Concr. Compos.* **2003**, *25*, 91−96.

(9) Juárez, C.; Duran, A.; Valdez, P.; Fajardo, G. Performance of "Agave Lecheguilla" natural fiber in Portland cement composites exposed to severe environment conditions. *Build. Environ.* **2007**, *42*, 1151−1157.

(10) Mehrez, I.; Hachem, H.; Gheith, R.; Jemni, A. Optimization of mortar/Agave Americana fibers composite behavior based on experimental design. *J. Nat. Fibers* **2023**, *20*, No. 2152149.

(11) Mancinoa, A.; Marannano, G.; Zuccarello, B. Implementation of eco-sustainable biocomposite materials reinforced by optimized agave fibers. *Struct. Integr. Proc.* **2018**, *8*, 526−538.

(12) Anandh, K. S.; Balasubramanian, M.; Stephen, P. An Experimental Study on Physical and Mechanical Properties of Agave Lechuguilla Fiber Used in the Concrete. *Adv. Nat. Appl. Sci.* **2016**, *10*, 442−448.

(13) Cao, Y.; Bao, J.; Zhang, P.; Sun, Y.; Cui, Y. A state-of-the-art review on the durability of seawater coral aggregate concrete exposed to marine environment. *J. Build. Eng.* **2022**, *60*, No. 105199.

(14) Mancinoa, A.; Marannano, G.; Zuccarello, B. Implementation of eco-sustainable biocomposite materials reinforced by optimized agave fibers. *Struct. Int. Procedia* **2018**, *8*, 526−538.

(15) Murtiadi, S. (2013). Properties Of Fibrous Lightweight Concrete Of Agave Sisalana.

(16) Betterman, L. R.; Ouyang, C.; Shah, S. P. Fiber-matrix interaction in micro fiber reinforced mortar. *Adv. Cem. Based Mater.* **1995**, *2*, 53−61.

(17) Sakuri, S.; Eko, S.; Dody, A.; Aditya, R. P. Investigation of Agave cantala-based composite fibers as prosthetic socket materials accounting for a variety of alkali and microcrystalline cellulose treatments. *Theor. Appl. Mech. Lett.* **2020**, *10*, 405−411.

(18) Ali, M.; Alabdulkarem, A.; Nuhait, A.; Al-Salem, K.; Almuzaiqer, R.; Bayaquob, O.; Algafri, Z.; et al. Thermal Analyses of Loose Agave, Wheat Straw Fibers and Agave/Wheat Straw as New Hybrid Thermal Insulating Materials for Buildings. *J. Nat. Fibers* **2021**, *18*, 2173−2188.

(19) Sathiamurthi, P.; Karthi Vinith, K. S.; Sathishkumar, T. P.; Arunkumar, S.; Anaamalaai, A. S. Fiber extraction and mechanical properties of Agave Americana/Kenaf fiber reinforced hybrid epoxy composite. *Mater. Today: Proc.* **2021**, *46*, 8594−8601.

(20) Deghboudj, S.; Boukhedena, W.; Satha, H. Optimization of Bending and Compressive Strength Behavior of Agave americana Fiber Reinforced Cementitious Composite Using Response Surface Methodology. *Period. Polytech., Civ. Eng.* **2023**, *67* (3), 744−756, DOI: 10.3311/PPci.21696.

(21) Caballero-Caballero, M.; Chinas-Castillo, F.; Montes Bernabé, J. L.; Alavéz-Ramirez, R.; Silva Rivera, M. E. Effect on compressive and flexural strength of agave fiber reinforced adobes. *J. Nat. Fibers* **2018**, *15* (4), 575−585.
(22) Cisneros-López, E. O.; González-López, M. E.; Pérez-Fonseca, A. A.; González-Núñez, R.; Rodrigue, D.; Robledo-Ortíz, J. R. Effect of fiber content and surface treatment on the mechanical properties of natural fiber composites produced by rotomolding. *Compos. Interfaces* **2017**, *24* (1), 35−53.
(23) Cisneros-López, E.; Pérez-Fonseca, A. A.; Fuentes-Talavera, F. J.; Anzaldo, J.; González-Núñez, R.; Rodrigue, D.; Robledo-Ortíz, J. R. Rotomolded polyethylene-agave fiber composites: Effect of fiber surface treatment on the mechanical properties. *Polym. Eng. Sci.* **2016**, *56* (8), 856−865.
(24) Bezazi, A.; Belaadi, A.; Bourchak, M.; Scarpa, F.; Boba, K. Novel extraction techniques, chemical and mechanical characterisation of Agave americana L. natural fibres. *Composites, Part B* **2014**, *66*, 194−203.
(25) ASTM D790 − 10 Standard Test Methods for Flexural Properties of Unreinforced and Reinforced Plastics and Electrical Insulating Materials,DOI: DOI: 10.1520/D0790-10.
(26) Wang, N.; Ding, E.; Cheng, R. Thermal degradation behaviors of spherical cellulose nanocrystals with sulfate groups. *Polymer* **2007**, *48* (12), 3486−3493.
(27) Mehrez, I.; Hachem, H.; Jemni, A. Thermal insulation potential of wood-cereal straws/plaster composite. *Case Stud. Constr. Mater.* **2022**, *17*, No. e01353.
(28) Msahli, S.; Sakli, F.; Drean, J. Y. Study of textile potential of fibres extracted from Tunisian Agave Americana L. *AUTEX Res. J.* **2006**, *6* (1), 9−13.
(29) Sgriccia, N.; Hawley, M. C.; Misra, M. Characterization of natural fiber surfaces and natural fiber composites. *Composites, Part A* **2008**, *39* (10), 1632−1637.
(30) Rama Sreekanth, P.; Kanagaraj, S. Assessment of bulk and surface properties of medical grade UHMWPE based nanocomposites using Nanoindentation and microtensile testing. *J. Mech. Behav. Biomed. Mater.* **2013**, *18*, 140−151.
(31) Rosas-Díaz, F.; García-Hernández, D. G.; Mendoza-Rangel, J. M.; Terán-Torres, B. T.; Galindo-Rodríguez, S. A.; Juárez-Alvarado, C. A. Development of a Portland Cement-Based Material with Agave salmiana Leaves Bioaggregate. *Materials* **2022**, *15*, 6000.
(32) Koohestani, B.; Darban, A. K.; Mokhtari, P.; Yilmaz, E.; Darezereshki, E. Comparison of different natural fiber treatments: a literature review. *Int. J. Environ. Sci. Technol.* **2019**, *16*, 629−642.
(33) Msahli, S.; Jaouadi, M.; Sakli, F.; Drean, J. Y. Study of the mechanical properties of fibers extracted from Tunisian Agave americana L. *J. Nat. Fibers* **2015**, *12* (6), 552−560.
(34) Agopyan, V.; Savastano, H., Jr; John, V. M.; Cincotto, M. A. Developments on vegetable fibre−cement based materials in São Paulo, Brazil: an overview. *Cem. Concr. Compos.* **2005**, *27* (5), 527−536.
(35) Bentur, A.; Akers, S. A. S. The microstructure and ageing of cellulose fibre reinforced cement composites cured in a normal environment. *Int. J. Cem. Compos. Lightweight Concr.* **1989**, *11* (2), 99−109.
(36) Stapper, J. L.; Gauvin, F.; Brouwers, H. J. H. Influence of short-term degradation on coir in natural fibre-cement composites. *Constr. Build. Mater.* **2021**, *306*, No. 124906.
(37) Faruk, O.; Bledzki, A. K.; Fink, H.; Sain, M. Biocomposites reinforced with natural fibers: 2000e2010. *Prog. Polym. Sci.* **2012**, *37* (11), 1552−1596, DOI: 10.1016/j.progpolymsci.2012.04.003.
(38) Li, Y.; Mai, Y. W.; Ye, L. Sisal fibre and its composites: a review of recent developments. *Compos. Sci. Technol.* **2000**, *60*, No. 2037.
(39) Onuaguluchi, O.; Banthia, N. Plant-based natural fibre reinforced cement composites: A review. *Cem. Concr. Compos.* **2016**, *68*, 96−108.

https://doi.org/10.1021/acsomega.3c03687
ACS Omega 2024, 9, 8743−8753